Influence of the cooling process on the physicochemical properties of ladle furnace slag, used in the replacement of Portland cement

Influência do processo de resfriamento nas propriedades físico-químicas da escória de forno panela, utilizada na substituição do cimento Portland

Tayná Fracão da Silva[1] , Marinara Andrade do Nascimento Moura[1] , Everton de Freitas Cordova de Souza[1] , Gisleiva Cristina dos Santos Ferreira[1,2] , Vanessa Ferreira Roche Pereira[2]

[1]Universidade Estadual de Campinas, Faculdade de Engenharia Civil, Arquitetura e Urbanismo. Rua Saturnino de Brito, 224, 13083-889, Campinas, SP, Brasil.

[2]Universidade Estadual de Campinas, Faculdade de Tecnologia. Rua Paschoal Marmo, 1888, 13484-332, Limeira, SP, Brasil.

e-mail: t261851@dac.unicamp.br, m228048@dac.unicamp.br, e233480@dac.unicamp.br, gisleiva@unicamp.br, vanessarochee@hotmail.co

ABSTRACT

Ladle furnace slag is a waste composed essentially of quicklime or hydrated lime, whose contents depend on the raw material and the cooling process that led to the slag batch. With this chemical composition, it is used by civil construction as a hydraulic binder in cement matrices. The chemical compounds mentioned are also present in Portland cement, which are part of the chemical reactions of hydration and hardening. However, the quality of LFS batches calls for attention to volume expansion caused by chemical compounds whose presence and content can be controlled by the cooling method adopted in the production. Considering the use of this material as a partial replacement for Portland cement, the objective of this study was the physicochemical characterization of LFS samples to evaluate the influence of the cooling method on its potential as a complementary binder in cementitious matrices. In this sense, 3 samples from different batches were analyzed and the effects of each cooling process. The results include analysis of specific mass, laser diffraction for particle size analysis, X-ray fluorescence and X-Ray Diffraction tests. It was verified that the sample obtained by slow cooling is the most suitable as binder, as it features less possibility of expansive chemical reactions and presents greater fineness.

Keywords: Ladle furnace slag; Cooling process; Cement replacement; Sustainable binder; Waste recycling.

RESUMO

A escória de forno panela é um resíduo composto essencialmente por cal virgem ou cal hidratada, cujos teores dependem da matéria-prima e do processo de resfriamento que deu origem ao lote de escória. Com essa composição química, ela é utilizada pela construção civil como aglomerante hidráulico em matrizes cimentícias. Os compostos químicos citados também estão presentes no cimento Portland, que fazem parte das reações químicas de hidratação e endurecimento. No entanto, a qualidade dos lotes EFP requer atenção à expansão de volume, causada por compostos químicos cuja presença e teor pode ser controlada pelo método de resfriamento adotado na produção. Considerando o uso deste material em substituição parcial ao cimento Portland, o objetivo deste estudo foi a caracterização físico-química de amostras de EFP para avaliar a influência do método de resfriamento em seu potencial como aglomerante complementar em matrizes cimentícias. Neste sentido foram analisadas 3 amostras de diferentes lotes e os efeitos de cada processo de resfriamento. Os resultados incluem análise de massa específica, difração de laser para análise de tamanho de partícula, fluorescência de raios X e testes de difração de raios X. Verificou-se que a amostra obtida por resfriamento lento é a mais indicada como aglomerante, pois apresenta menor possibilidade de reações químicas expansivas e apresenta maior finura.

Palavras-chave: Escória de forno panela; Processo de resfriamento; Substituição de cimento; Aglomerante sustentável; Resíduo reciclável.

1. INTRODUCTION

The steel industry is responsible for generating several types of solid waste. One of this type is the Ladle Furnace Slag (LFS), which is originated from the secondary refining of steel. The steel world production is around 1.95 billion tons per year and, for each ton of steel produced, 30 to 50 kg of LFS are generated [1, 2]. Annually, it is generated about 30 million tons of LFS [3]. The environmental and economic impacts, resulting from the volume generated and the financial costs for the destination in sanitary landfills, direct the search for sustainable alternatives for the use of uses as complementary binders are mainly based on the presence of oxides commonly found in Portland Cement such as CaO, SiO_2, Al_2O_3 and MgO [4, 5]. However, the granular characteristics of most LFS batches direct the studies to the use as an aggregate (coarse or fine), which ends up reducing the added value that this residue can represent [6–8].

Regarding the LFS granulometry, the cooling processes directly interfere in this physical characteristic. These methods are defined by the steel industry, during the stages of steel production, depending on the raw material available and technologies adopted, and can be classified as slow or fast [9]. Slow cooling occurs from the contact of the slag with moisture in the air, while rapid cooling occurs by spraying water on the material, causing a thermal shock [10, 11]. In slow cooling, the chemical reactions of transformation of larnite (βC_2S) into belite (γC_2S) stand out. The belite presents greater expandability (increase of 10% in relation to the initial total volume) causing internal tensions, which provide the continuous fragmentation of the LFS grains. This physicochemical process results in the refinement of the slag batches, that is, producing a finer material [12, 13].

Another problem reported in the bibliography is the possible expansive chemical reactions, which occur due to the presence of lime and periclase. LU *et al.* [14] describe that slow cooling produces LFS samples with lower content of free CaO and MgO than the one found for samples produced by fast cooling. The low content of these oxides reduces the possibility of expansive hydration reactions. This method provided cementitious mixtures with the incorporation of LFS and expansion volume 10% lower than the samples produced with water cooling [9, 10, 15–17]. Therefore, slow cooling can benefit LFS both in terms of granulometry (greater fineness) and in terms of reducing expansive chemical reactions.

Even so, up to now most of the research available in the literature does not report the type of cooling that the LFS samples used were submitted to. As there is no such concern, several studies report the non-viability of using this type of slag as a complementary binder, which could be reversed if these LFS batches were selected according to the cooling method.

Considering that the functionality of LFS batches essentially depends on the raw material and cooling method used by the steel industries, it is verified that it is essential to know their physicochemical characteristics. Therefore, the objective of this research was the physicochemical characterization of three LFS samples, with different cooling methods, seeking their suitability as a secondary binder in cementitious matrices.

2. MATERIALS E METHODS

2.1. Materials

This study used three different samples of LFS, water and high initial strength Portland cement (CP-V ARI) to produce cement pastes. The LFS samples were produced in different units of the same Brazilian steel company, having also been submitted to different cooling conditions. Sample A1 was obtained by slow cooling with air in the Brazilian state of São Paulo, sample A2 was cooled with a controlled volume of water, in Minas Gerais State, and sample A3 was rapidly cooled with high-pressure water jets and originated in the Espírito Santo State.

2.2. Methods

Due to the granulometric heterogeneity of the samples, resulting from the different cooling methods, it was necessary to carry out their pre-processing. For this, the portion retained on the #1.18 mm sieve was ground to be later subjected again to the same sieving after that, as shown in Figure 1 [6]. A MA500 mill was used with an alumina ceramic jug (1l capacity) and 40 ceramic balls of 20 mm in diameter, with cycles of 15 minutes and 200 rpm speed for each 400 g of slag. Figure 2 shows the visual characteristics of the three samples before and after processing.

After pre-processing the LFS samples, this material and cement were characterized by the following methods: specific mass test was performed according to NBR 16605 [18]. For the particle size analysis, the Mastersizer 2000 equipment was used, with samples of 0.15 g of LFS in a 50 ml solution, dissolved with the aid of a RW20 overhead stirrer (IKA) and rotation at 1000 rpm for 1 minute. The X-Ray Fluorescence (XRF) analyzes
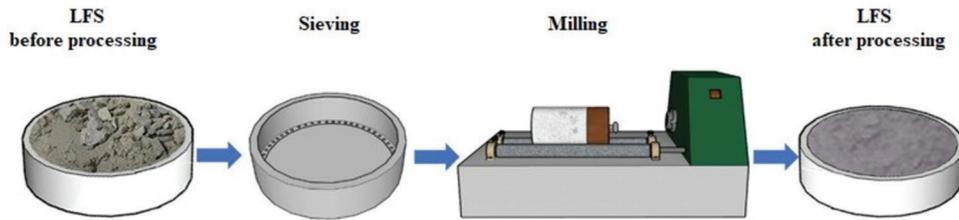
Figure 1: Processing steps for LFS samples.
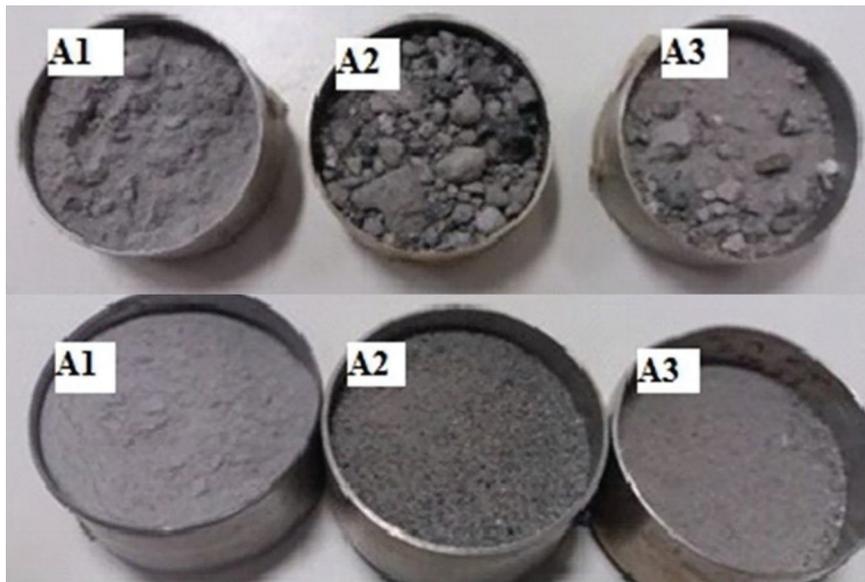
Figure 2: LFS samples before (top) and after (bottom) the sieving and milling.

were performed with LFS samples pressed in the STD-1 (Standardless) calibration, considering chemical element standards in the range between fluorine and uranium. Loss of ignition (LI) was obtained after exposing the 3 samples in a heated oven at 1.200ºC for 2 h. For X-Ray Diffraction (XRD) analysis, a voltage of 40 kV, current of 40 mA, with a 2theta interval from 5 to 100°C and speed of 0.0166 °C/s were used. The crystalline phases were obtained by comparing the samples diffractograms with PDF2 databases from the International Center for Diffraction Data – ICDD (2003) and PANalytical Inorganic Crystal Structure Database – PAN-ICSD (2007). To study microstructure of LFS were realized in a scanning electronic microscopy equipped with energy dispersive X-rays microscopy (SEM/EDX) model VEGA 3 SEM, TESCAN.

In order to evaluate the basic hydration potentials of the samples, cementitious pastes were produced and initially subjected to a thermally insulated system so that the heat released in the hydration of the binders was quantified directly by monitoring the heat flux generated by the paste, allowing the determination of the calorimetry curves. These rates were used to verify the viable cement replacement content.

Thus, the reference paste (PA REF) was produced with conventional mix without replacement, as the other three had 30% replacement of portland cement by samples A1, A2 and A3, named respectively PA1, PA2, and PA3. The proportion of water was defined seeking a normal consistency for NBR 16606 [19], where the respective values of 31.7%, 37.2%, 26.6%, and 29.2% were obtained. This replacement was defined based on the positive results presented by HERRERO *et al.* [20].

The mechanical behavior of the reference and LFS pastes was investigated through the compression and bending test, at 28 days age (NBR 13279 [21]). The expansion index was obtained by Le Chatelier Test (NBR 16697 [22]) and, X-ray Diffraction (XRD) and thermogravimetric tests were also performed to obtain main chemical compounds, results of the Portland cement+LFS hydration. The results obtained were analyzed to determine values of variability, null hypothesis, and scatters. This analysis of statistical significance was performed using the ANOVA method and the Tukey Test using the OriginPro Software.

3. RESULTS AND DISCUSSON

3.1. Materials characterization

3.1.1. Physical analysis

The physical characterization of the LFS and cement samples is shown in Figure 3 and Table 1. The samples had their specific masses of 2.76, 3.07 and 2.98 g/cm³, respectively, values close to that of Portland cement (3.12 g/cm³). Considering the similarity of this physical property between the two and the effect it exerts on the cement binding potential, it is directed to the comparison of the values of the three samples of LFS with the literature. An interval was found close to that found in this study (2.75 to 3.6 g/cm³) [10, 20, 23], confirming that the use of this slag as a secondary binder is feasible.

The difference between the specific mass of the samples of LFS studied comes from the cooling methods to which they were submitted. In addition to storage time and chemical composition, the cooling method is highlighted as a determining factor to define the physicochemical properties of this type of slag [20, 23, 24]. ILDIRIM and PREZZI [25] also identified similarities between specific mass to storage time (slow cooling), that is, longer cooling time results in lower specific mass of the LFS. This can be justified due to the high content of calcium oxides (CaO), which when in contact with ambient humidity and carbon dioxide (CO_2), hydrate and form hydrated lime (Ca $(OH)_2$), a chemical compound with less mass molecular [20, 24].

In contrast, fast cooling (with water), provides greater trapping of water or air in the LFS particles, which consequences are greater water absorption and greater specific mass [10]. This can be verified by the
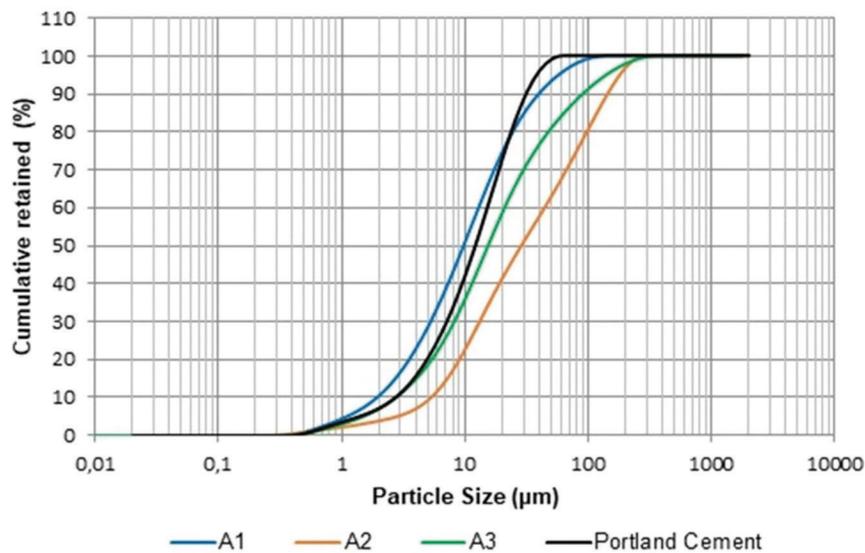
Figure 3: Particle size curve of Portland cement and LFS samples.

Table 1: Specific mass of LFS and Portland cement samples.

RESULTS	A1	A2	A3	PORTLAND CEMENT	SETIÉN *et al.* [24]	PAPAYIANNI AND ANASTASIOU [6]
Specific mass (g/cm³)	2.76	3.07	2.98	3.12	–	–
Average diameter (μm)	18.46	52.40	35.22	–	–	–
D (0.1) (μm)	2.15	2.71	2.78	2.69	3.00	3.5–10
D (0.5) (μm)	10.91	20.66	17.24	12.01	–	70–90
D (0.9) (μm)	44.57	157.45	93.23	31.07	55	20–150

D (0.1) – Diameter corresponding to 10% of the passing material.
D (0.5) – Diameter corresponding to 50% of the passing material.
D (0.9) – Diameter corresponding to 90% of the passing material.

characteristics of sample A1, which was obtained by the slow cooling process and presented a smaller average diameter (18.5 μm) compared to samples A2 (DM = 52.4 μm) and A3 (DM = 35.22 μm).

The slags this research has smaller grains, when compared to the results obtained by HENRÍQUEZ *et al.* [26], whose slag sample showed a particle size between 0–2000 μm. This difference is attributed to the previous processing adopted (sieving and grinding) and to the characteristics of the industrial processes that originated this samples. Thus, by considering the use of LFS in cementitious matrices, granulometry is a very important parameter, as it directly interferes with the rheological properties of this type of material, since the greater the fineness of the slag (specific surface), the lower the viscosity [27].

3.1.2. Chemical Analysis

Table 2 shows the mineral composition of the LFS samples and Portland cement obtained with XRF analysis. The main oxides present in LFS samples (CaO, SiO_2; Fe_2O_3; MgO) are also included in the chemical composition of Portland cement. The high levels of calcium oxide in the three samples can be explained by chemical additions occurred during the refining process of metal alloys, for example, calcium fluoride (CaF_2) [28]. When comparing the chemical composition of the samples, it is verified that the magnesium oxide content is similar (6.82 at 8.80). Regarding the iron oxides, sample A2 has a greater amount (26.8%), when compared to the other two samples. This characteristic is linked to the production methodology of each industry, that is, by increasing the presence of these oxides, the loss of raw material in the refining process is boosted.

Regarding the calcium and magnesium oxides, some researchers emphasize that the levels must be controlled, especially MgO, as they present expansive chemical reactions in the presence of water, which can affect the physical stability of cementitious matrices with LFS incorporation [25, 29–31]. Calcium oxides can generate quick expansive reactions due to their immediate hydration process. Differently, magnesium oxides react more slowly, resulting in late expansion [30].

Discussions about the chemical composition of LFS samples lead to the conclusion that the method of cooling these slags directly influences their hydraulic properties. Slow cooling stands out due to supply of hydration of CaO with ambient humidity, reducing the possibility of expansive reactions when present in cementitious matrices [10].

Another characteristic that differentiates sample A1 from samples A2 and A3 is the mass loss after high temperature. The sample A1 (slow cooling) showed loss on ignition (LOI: 14.5%) whereas samples A2 and A3, that showed gain on ignition (GOI). This phenomenon results from the oxidation of ferrous minerals present in the material [32, 33]. The LFS sample used by BRAVO and SILVA [33] also presented GOI, justified by the oxidation of aluminum and iron present, which have a higher density.

The images obtained with the Scanning Electron Microscope (SEM) are shown in Figure 4. Through the images it is possible to identify the granulometric differences of the 3 LFS samples, confirming the interference of the cooling method on the fineness of the slag. It is also possible to identify that samples A1 and A3 present a small percentage of grains with more irregular shapes than sample A2, resulting by the respective cooling process and greater presence of ferrous minerals in sample A2. This can be explained by the respective cooling processes and greater presence of ferrous minerals in sample A2. This test also allows the identification of the main chemical compounds of the samples with a spectrogram, obtained with Energy Dispersive X-Ray Analysis (EDX), quantified from the X-Ray Fluorescence test (XRF), whose values are presented in the Table 3.

Table 2: Content of chemical elements present in samples of LFS and Portland cement, obtained with XRF analysis.

SAMPLES	CHEMICAL COMPOUNDS (%)									
	CaO	Fe_2O_3	SiO_2	MgO	MnO	Al_2O_3	SO_3	F	CaO/Al_2O_3+- SiO_2	LOI (%)
A1	54.20	3.40	11.50	8.80	2.68	1.32	1.93	0.59	4.22	14.5
A2	35.60	26.80	18.00	8.03	1.89	4.13	2.11	1.52	1.60	GOI
A3	52.30	14.50	16.50	6.82	1.12	3.28	1.78	1.93	2.64	GOI
Portland cement	61.90	2.47	17.30	2.97	0.06	4.04	2.97	–	–	5.70
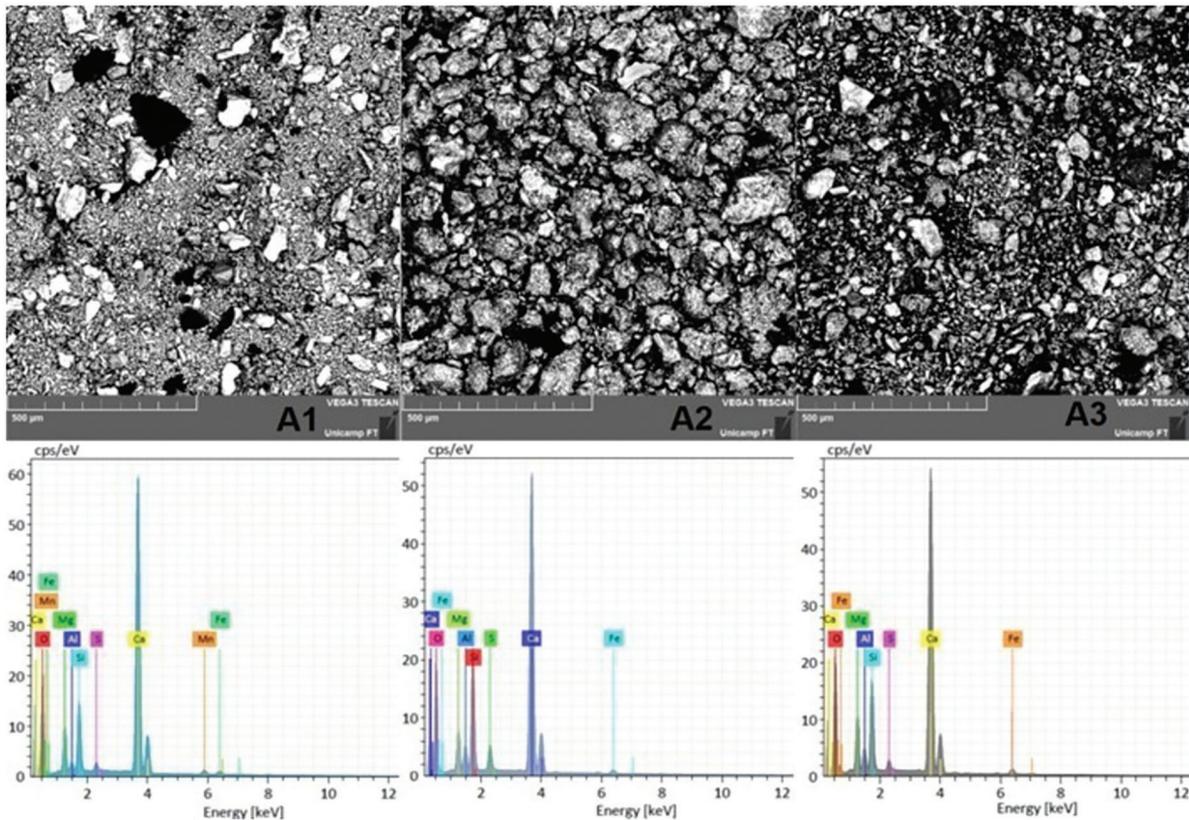
Figure 4: Microstructure images of LFS samples obtained with SEM and mineralogical data from EDX analysis.

Table 3: Main chemical compounds of the LFS samples.

SAMPLES	CHEMICAL COMPOUNDS (%)							
	O	**Mg**	**Al**	**Si**	**S**	**Ca**	**Mn**	**Fe**
A1	50.66	4.64	0.70	4.31	0.56	37.19	1.05	0.88
A2	52.71	3.73	1.91	6.37	1.73	32.63	–	0.91
A3	53.66	4.96	1.68	5.05	0.63	32.60	–	1.42

SEM/EDX characterization of LFS samples shows high Ca content, small amounts of Si and Mg, in addition to some traces of other elements (Al, S, Fe and Mn), which are commonly found in slag. According to the diffractograms in Figure 5, no amorphous halos were identified in the 3 LFS samples, on the contrary, it was possible to identify several crystalline compounds (Calcium Silicate, Portlandite, Calcite, Quartz, Periclasium and Cuspidine), also present in Portland cement and mineral additions. The minerals present in the three LFS samples were also identified in samples from similar studies that analyzed this material, the correspondences are listed in Table 4 [20, 26, 34].

The diffractogram peaks of the most frequent crystalline compounds were identified as calcium disilicate ($Ca_2(SiO_4)$), which can be divided into olivine and larnite [24]. These compounds can develop hydraulic properties under adequate conditions of temperature and humidity, highlighting that larnite is considered more reactive than olivine. As mentioned above, LFS compounds identified as larnite are transformed into olivine when the slow cooling process generates the slag. Despite the lower reactivity, the greater presence of this last compound in LFS batches can reduce and even avoid expansive chemical reactions during the hydration process of the cementitious matrix [10]. As a solution, it might be indicating the use of pozzolanic additions (high content of silica and aluminum oxides), which chemically react with free CaO present in LFS, forming calcium silicate hydrated (C-S-H) [35]. The larger formation of this composite contributes to the increase in the performance of cementitious matrices, as it provides a gain in mechanical strength and, consequently, greater durability [6, 8].

Calcite ($CaCO_3$) and periclase (MgO), considered as free lime and free magnesium, respectively, are present in the 3 slags (A1, A2, A3) and in the samples studied by other authors [26, 34]. FRÍAS ROJAS and SÁNCHEZ DE ROJAS [36] report that these compounds present expansive chemical reactions, which can
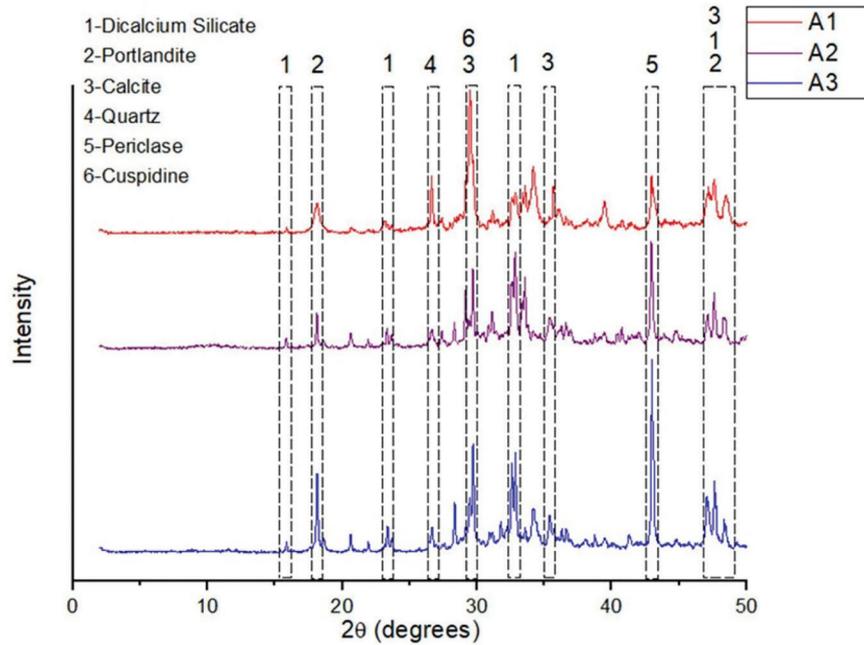
Figure 5: Mineralogical diffractogram of LFS samples.

Table 4: Mineralogical composition of raw materials.

MINERALOGICAL COMPOSITION (%)	MINERALOGICAL PHASE	A1	A2	A3	HENRÍQUEZ *et al.* [26]	MARINHO *et al.* [34]	HERRERO *et al.* [20]
$Ca_2(SiO_4)$	Calcium silicate	x	x	x	x	x	x
$Ca(OH)_2$	Portlandite	x	x	x	x	x	
$CaCO_3$	Calcite	x	x	x	x	x	
SiO_2	Quartz	x	x	x	x	x	
MgO	Periclase	x	x	x	x	x	x
$Ca_4Si_2O_7F_2$	Cuspidine	x	x	x			
Fe_3O_4	Magnetite		x	x		x	
CaF_2	Fluorite		x	x		x	x
$Mg(OH)_2$	Brucite		x	x	x	x	x
$Ca_3Mg(SiO_4)_2$	Merwinite	x	x		x	x	x
$Ca_3(SiO_4)O$	Calcium silicate			x			x

generate cracks in the cement matrix, arising from internal tensions. Contrarily, Brucite ($Mg(OH)_2$), present in samples A2 and A3 demonstrates lower potential for expansion.

Due to the low concentration of iron oxide (FeO) in sample A1 (3.4%), only samples A2 and A3 have the compound Magnetite (Fe_3O_4), identified in the XRD analysis. It is noteworthy that the lower index of this compound is a characteristic of this type of steel slag. Some authors verified that LFS has, on average, 10% less iron oxides in its composition, when compared to Blast Furnace Slag and Basic Oxygen Furnace Slag [37].

SETIÉN *et al.* [24] point out that the higher ratio between calcium oxide and aluminum and silica oxides ($CaO/Al_2O_3+SiO_2$) (Table 2), indicates the lower content of the compound mayenite ($Ca_{12}A_{14}O_{33}$), a type of calcium aluminate. Some studies describe that this relationship ranged between 1 and 2 [6, 38], which was well below the relationship presented by sample A1 (4.22). It is important to mention that the identification of mayenite in LFS samples is related to the high concentrations of aluminum added during the deoxidization process of the secondary refining of steel in the ladle furnace slag [28]. Nonetheless, in this study samples, calcium fluoride (CaF_2) is used in this process, justifying the absence of this calcium aluminate. The interaction of the raw material (according to the region of waste production) with the cooling method, allows several combinations, which defines a gap in the study that relates these factors.
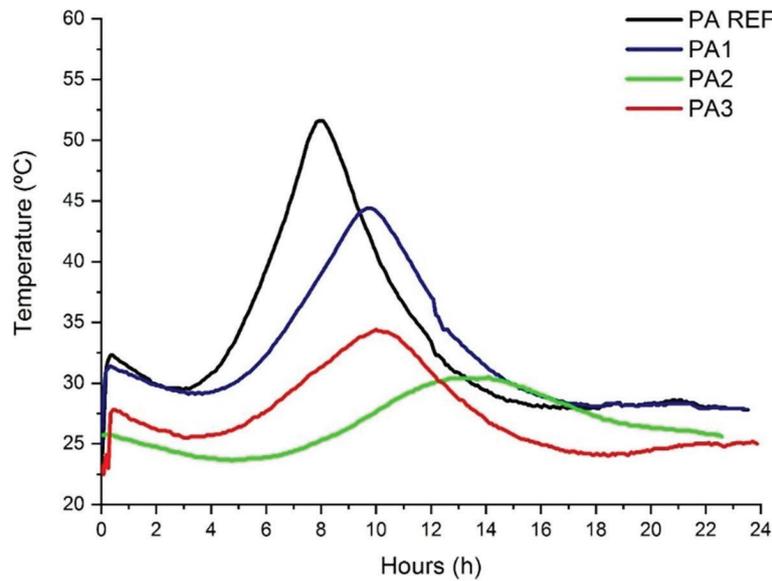
Figure 6: Hydration curves of the cementitious pastes.

3.2. Cementitious pastes characterization

3.2.1. Calorimetry analysis

As reported in Chapter 2, the hydration curves of cementitious pastes were obtained with the 3 samples of LFS studied, fixing the content of 30% in substitution of Portland cement (Figure 6).

Already studied by other authors [39, 40], the evolution of hydration of hydraulic binders can be qualified from the relationship between time (h) and heat release (°C). Among the various information that can be collected from the calibration curve, the start and end times of setting, in addition to the corresponding temperatures, stand out. In the specific study, it is also possible to compare the behavior of the pastes with LFS and the reference paste (100% PC), and verify the hydraulic properties of this type of slag in the presence of PC and water. The curves of the pastes with replacement of Portland cement by LFS, showed a lower heat of hydration in relation to the curve of the reference paste. However, among the pastes with LFS, PA1 presented the best performance in relation to the reference paste, that is, the maximum hydration temperature was only 20% lower than the REF paste. This can be attributed to the fineness of the A1 sample (D0.5 = 10.91 µm), associated with the chemical composition (XRF and XRD). The intensity of the calcite peaks (Figure 5) indicates that sample A1 has a higher reactivity potential, which coincides with observations by other authors [9, 10, 20].

3.2.2. Compressive and flexural strength

The mechanical behavior of the reference and LFS pastes was investigated through the simple compressive and flexural strength are presented on Table 5, as well as the descriptive statistical analyses. The Figure 7 explained statistically analyze the data, comparing pastes between pairs, to verify if there is statistical equality.

Table 5: Compressive and flexural strength of the reference and experimental pastes.

IDENTIFICATION	PA REF	PA1	PA2	PA3
Compressive Strength (MPa)	64.17	46.02	56.66	59.28
Standard deviation (MPa)	11.10	4.87	3.57	4.13
Coefficient of variation (%)	17.30	10.59	6.31	6.96
P-value			0.0011	
Flexural Strength (MPa)	8.42	7.37	10.12	7.33
Standard deviation (MPa)	0.36	1.30	0.75	0.60
Coefficient of variation (%)	4.33	17.71	7.43	8.25
P-value			0.0106	
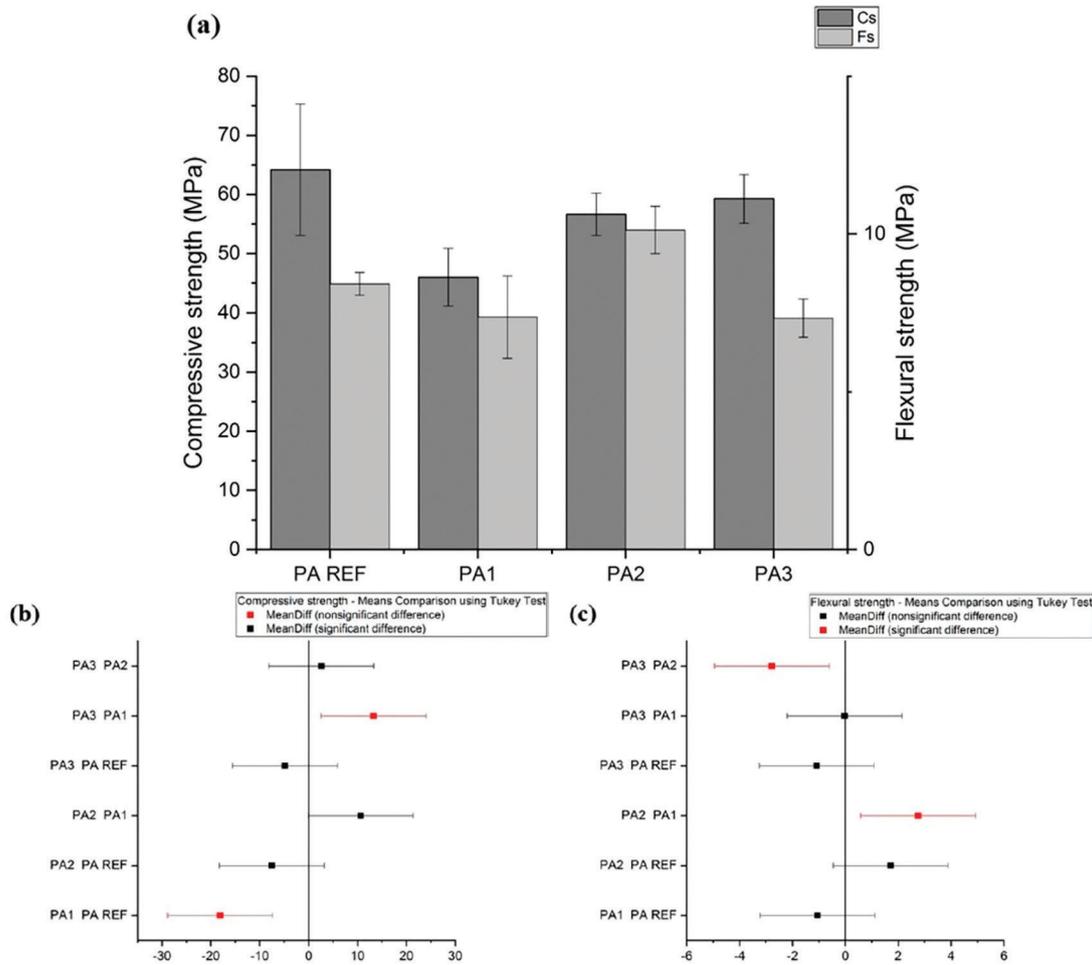
Figure 7: Compressive and flexural strength identified in the pastes (a), along with by statistical significance tests (b).

The mechanical results of pastes showed that there was a reduction in mechanical properties, mainly in relation to compressive strength. It was expected that 30% replacement of PC would result in this behavior, most because the chemical reactions of LFS are slower, and results were obtained with 28 days of curing. Regarding compressive strength, the REF paste is statistically equal to PA2 and PA3 pastes. As for the tensile strength, all pastes with slag were statistically equal to REF paste.

Despite this, it should be noted that the mechanical properties of cementitious materials, with the incorporation of LFS as a binder, should be evaluated at more advanced ages, considering the speed of the chemical reactions of hydration. SANTAMARIA *et al.* [41] and PARRON-RUBIO *et al.* [42] explain that the reduction in the mechanical strength of cementitious materials with LFS is mainly due to the silica and aluminum contents. When verifying such chemical elements in the samples of the present study, it appears that the Si contents are compatible with those presented by the PC (18% and 16.5% for A2 and A3, respectively) and 17% for the PC. However, sample A1 has only 11.5% of Si, which may explain the lower compressive strength in relation to the others. Regarding the Al_2O_3 contents, only the A2 sample presented a value like that of the PC (4.04 and 4.13, respectively).

3.2.3. Expansion rates

The values for the expansion test at 7 days are shown in Table 6. Figure 8 displays the results of expandability and the statistical analysis (ANOVA and Tukey Test).

It is established that the expandability of Portland cement with or without additions is less than 5 mm (NBR 16697 [22]). The greatest expandability presented by the pastes studied in this work was 3.3 mm (A3S30). Therefore, it appears that all pastes meet the maximum expandability value, despite the afore mentioned pastes presenting values higher than the REF paste (cement only). The presence of calcium and magnesium in the three samples induces a volumetrically unstable behavior, handled in this research by the lowest

Table 6: Expandability rates identified in the reference and experimental pastes.

IDENTIFICATION	PA REF	PA1	PA2	PA3
Expandability (mm)	1.30	2.30	3.00	3.30
Standard deviation (mm)	0.58	0.58	0.01	0.58
Coefficient of variation (%)	43.30	24.74	33.33	17.32
P-value	0.0362			
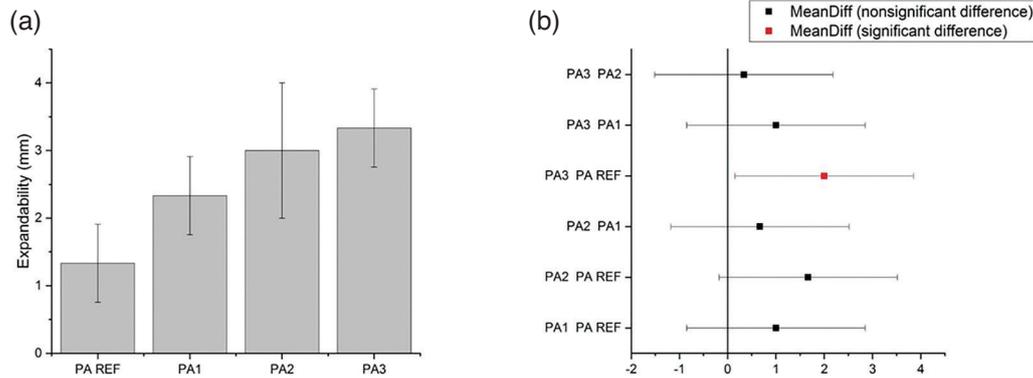
Figure 8: Expansion rates measured in the pastes (a) along with the statistical significance tests (b).

applied content [34]. However, it is difficult to obtain the percentage of these chemical elements that are still reactive, that is, free in the slag, and with greater reactivity, consequently causing greater expandability. It is noteworthy that calcium exhibits greater expandability due to the speed of hydration, while magnesium oxides chemically react more slowly, resulting in delayed expansion [30]. It is noteworthy that the expandability of cement matrices with LFS must be determined at advanced ages, identifying possible performance and durability problems [36]. Samples of LFS with 55% of CaO had this content reduced to 1%, after being used in mortar, the requirement of the European standard EN 450, which meeting the maximum limit at 2.5% to reduce the risk of expandability [6].

3.2.4. Thermogravimetric Analysis (TGA)

Thermogravimetric analysis (TG) allows the quantification of important compounds in the pulp, such as the content of hydrates formed, portlandite consumed during hydration reactions and carbonation of the pulp [43]. Figure 9 shows TGA curves (derived from thermogravimetry) of PA REF, PA1, PA2 and PA3 pastes, respectively. By analyzing these figures, it is possible to identify five main peaks, which indicate the most important changes, which were classified by temperature ranges (5 ranges).

The first mass loss (range 1) occurs from 30 to 150°C, and is associated with the loss of free, adsorbed, and combined water. The last 2 are related to C-S-H [43–49]. Up to 170°C decomposition of gypsum and ettringite can also occur. According to A, the pastes with lower mass loss indicate the lack of free water in the mixture and the absence (or lower frequency) of the ettringite compound in the microstructure [44]. The second mass loss (range 2) occurs from 300 to 350°C and is associated with the mass loss of magnesium hydroxides [Mg (OH)$_2$] [48, 50] while the third, range 3, occurs from 400 to 450°C and is associated with dehydration of portlandite [Ca(OH)$_2$] [43–45, 48]. Finally, the fourth (range 4) and fifth (range 5) mass losses, which occur from 600 to 650°C and 730 to 820°C, respectively, are associated with decarbonation of calcite [CaCO$_3$] [43, 44, 47–49].

To compare the behavior of the pastes Figure 10 and Table 7 were created, where it was possible to obtain the mass loss (%) in each temperature range identified in the Figure 9. When comparing the pastes with LFS (1, 2 and 3) and the REF paste, it can be seen that: the 3 pastes with LFS present similar mass loss in range 1 (30 °C to 150°C), varying between them 0.77 %. In range 2 (330°C to 350°C) it is observed that the values of mass loss referring to magnesium hydroxide (Mg (OH)$_2$) were similar between PA1 and PA2 pastes and REF paste. This indicates that the formation of expansive compounds, resulting from the hydration of MgO, is practically the same for this curing time (28 days). Only PA3 paste presented lower mass loss in this range, justified by the lower
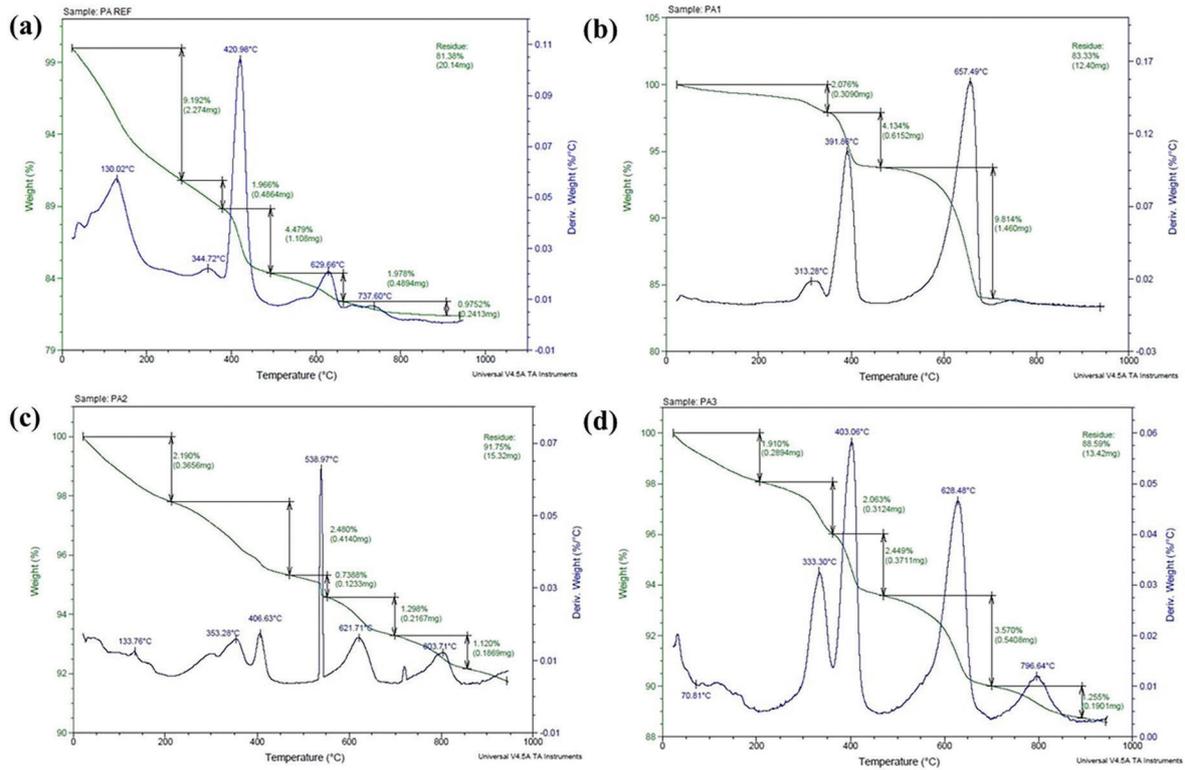
Figure 9: Thermogravimetric analysis of the reference paste (a), PA1 (b), PA2 (c), and PA3 (d).
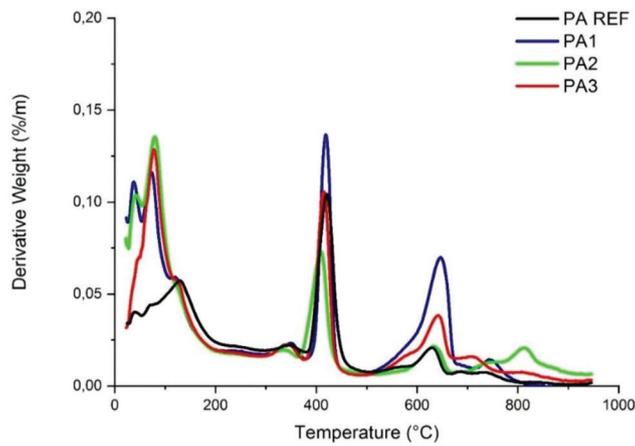
Figure 10: Comparative thermogravimetric analysis of reference and experimental pastes.

Table 7: Mass loss in the samples identified in the Isothermal calorimetry analysis.

		MASS LOSS (%)			
RANGE	TEMPERATURE (ºC)	PA REF	PA1	PA2	PA3
1	30–160	9.19	12.53	13.30	12.02
2	330–350	1.96	2.11	1.89	1.67
3	400–450	4.47	4.12	3.58	3.69
4	600–650	1.97	5.58	1.98	5.24
5	730–820	0.97	0.97	2.98	–

MgO content (6.82%). It leads to the conclusion that the expansibility shown in Figure 8 is the result of expansive reactions with free CaO.

In range 3 (410°C to 450°C), where the dehydration of portlandite (Ca (OH)$_2$) occurs, the mass loss of PA1 paste was greater than that of the other pastes with LFS, and similar to the loss presented by the REF paste. This behavior leads to the conclusion that portlandite contents are maintained between PA1 and REF pastes, even with a 30% reduction in PC, which confirms the hydraulic properties of this type of slag.

The decarbonation of calcite in ranges 4 and 5 (590 to 820°C) presents greater mass loss for PA1 paste, when comparing others pastes with LFS and paste REF. This behavior indicates that the CaO content resulting from the previous range (3) is higher for the PA1 paste, which can be explained by the higher (Ca (OH)$_2$) content of this slag, which reduces the possibility of C-S-H formation during the period of hydration. One option to improve the performance of LFS as a hydraulic binder is the use of pozzolanic additions in cementitious materials with LFS.

3.2.5. XRD analysis

To identify the main minerals presents in the cementitious pastes, obtained XRD analysis, presented the Figure 11. Table 8 presents the main peaks and their identification.
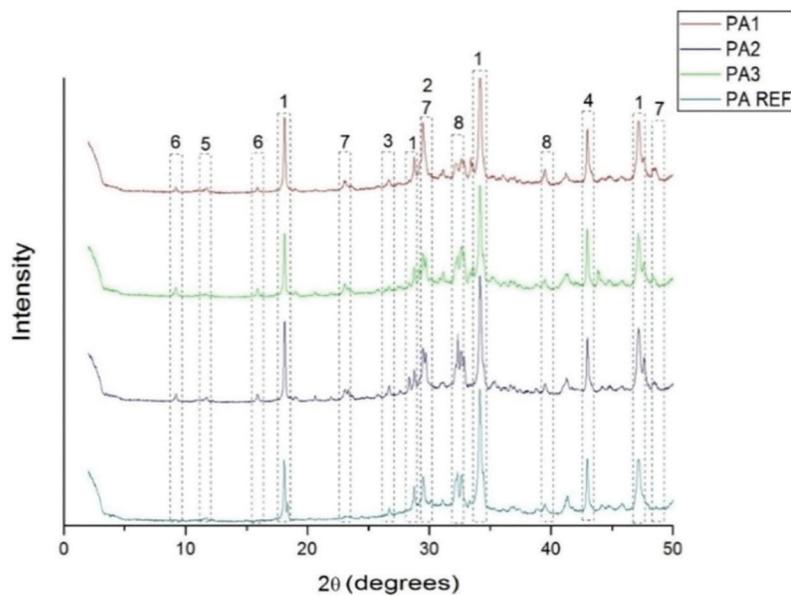
Figure 11: Mineralogical diffractogram of reference and experimental pastes.

Table 8: Chemical compounds identified in the pasts through XRD Analysis.

NUMBER	COMPOUND	CHEMICAL FORMULA	PA REF	PA1	PA2	PA3
1	Portlandite	Ca (OH)$_2$	x	x	x	x
2	Calcite	CaCO$_3$	x	x	x	x
3	Quartz	SiO$_2$	x	x	x	x
4	Periclase	MgO	x	x	x	x
5	Gypsum	Ca$_2$H$_2$O	x	x	x	x
6	Etringite	Ca$_6$A$_{12}$(SO$_4$)$_3$(OH)$_{12}\cdot{}_{26}$H$_2$O		x	x	x
7	Olivine	Ca$_2$(SiO$_4$)		x	x	x
8	Larnite	Ca$_2$(SiO$_4$)		x	x	x

Representing the most prominent peak, Portlandite showed similarity of the three experimental mixtures to each other and to the reference. This compound demonstrates the hydration of lime present in both Portland cement and LFS. Less intense portlandite rates on XRD images indicate that the hydrate is being consumed during the reaction and formation C-S-H [51]. Calcite demonstrated relevant indexes as well. Coming from the calcium used in tempering processes in steel industries, it is also from the conventional Portland cement, where it is a main constituent. By being an inert and anhydrous material, it does not present chemical significance in the hydration reactions of the paste [9].

In contrast, periclase is a noteworthy compound due to its expansive influence in the matrix behavior. Identified in all cementitious pastes including the reference one, it is due to the presence of magnesium in the slag composition and in the natural occurrence of this compound in the limestone rocks used for the manufacture of cement [17]. Sample A3, which presented better performance in compressive strength analysis, also presents lower periclase peaks than the others. It can also be observed that the periclase peaks diffracted in the sample 3 appear close to the diffracted peaks of the reference paste. It is important to remember that sample 3 has a lower content of magnesium in its chemical composition than the others, about 16% and 22.5% less than samples 2 and 1 respectively.

Another worrying compound is ettringite, with expansive properties that can lead to cracks and destabilize the cement matrix [17, 20, 34]. Diffracted in all pastes with LFS, this compound is formed both by the aluminates present in the cement composition (C2A and C3A) and by the aluminum present in the chemical analyzes of the samples (Table 2). However, it is worth mentioning the considerable decrease of this compound in the PA1 sample, due to the purity of the LFS sample used.

Finally, calcium silicate peaks were identified in all pastes in two different polymorphs (olivine and larnite). Dicalcium silicates existing in both slag and Portland cement, show crystallographic changes that stabilize at different temperatures. Due to this instability, its presence in the pastes slightly alters the overall hydration potential of the mixture, as already discussed in relation to the chemical composition of LFS samples.

4. CONCLUSIONS

The experimental analysis of the present work demonstrated the influence of the cooling process on the LFS batch, verifying that the sample submitted to slow air-cooling had fewer chemical compounds that trigger volume expansion.

The slow cooling sample (A1) might be more suitable to be used as a secondary binder in cementitious matrices, when compared the ones generated by controlled water and high-pressure water jets, since slow cooling generates slags with physicochemical properties that indicate a lower chance of expansive chemical reactions. The importance of characterizing batches of LFS prior to its use as a secondary binder is evidenced because the source of the raw material (scrap) and the material's cooling methods determine its characteristics.

In relation to cement pastes with LFS, the mechanical behavior does not directly identify sample A1 as the most appropriate to be used as a secondary or complementary binder. However, when analyzing other parameters, it is possible to conclude that the lower expandability, together with the DTA analyzes (chemical alterations), indicate better overall performance of this LFS sample.

This search for a better binding potential is emphasized This search as the sustainable advantages of its use are sought after for the sectors involved, in order to reduce cement consumption and the steel industry's environmental liabilities.

Suggestion for future studies include the exploration of sample A1 use in cementitious matrices together with a pozzolan. This sample presents greater availability of Ca $(OH)_2$, enables the formation of C-S-H, through pozzolanic reactions. In addition, to evaluate cementitious materials with a longer curing period (above 28 days).

5. ACKNOWLEDGEMENTS

6. REFERENCES

[1] WORLDSTEEL ASSOCIATION, *Total production of crude steel*, https://worldsteel.org/steel-by-topic/statistics/annual-production-steel-data, accessed in September, 2022.

[2] MAGHOOL, F., ARULRAJAH, A., DU, Y., *et al.*, "Environmental impacts of utilizing waste steel slag aggregates as recycled road construction materials", *Clean Technologies and Environmental Policy*, v. 19, n. 4, pp. 949–958, 2017. doi: http://dx.doi.org/10.1007/s10098-016-1289-6.

[3] MAHOUTIAN, M.*,* SHAO, Y., "Low temperature synthesis of cement from ladle slag and fly ash", *Journal of Sustainable Cement-Based Materials*, v. 5, n. 4, pp. 247–258, 2016. doi: http://dx.doi.org/10.1080/21650373.2015.1047913.

[4] PAUNA, H.*,* AULA, M.*,* HUTTULA, M., *et al.*, "Quantifying the CaO and CaF2 content of industrial ladle furnace slag with optical emissions measured through the casting spout.", *Steel Research International*, v. 93, n. 5, pp. 2100519, 2022. doi: http://dx.doi.org/10.1002/srin.202100519.

[5] XU, B.*,* YI, Y., "Treatment of ladle furnace slag by carbonation: carbon dioxide sequestration, heavy metal immobilization, and strength enhancement.", Chemosphere, v. 287, n. Pt 3, pp. 132274, 2022. doi: http://dx.doi.org/10.1016/j.chemosphere.2021.132274. PubMed PMID: 34562709.

[6] PAPAYIANNI, I.*,* ANASTASIOU, E., "Effect of granulometry on cementitious properties of ladle furnace slag", *Cement and Concrete Composites*, v. 34, n. 3, pp. 400–407, 2012. doi: http://dx.doi.org/10.1016/j.cemconcomp.2011.11.015.

[7] RODRIGUEZ, Á.*,* MANSO, J.M.*,* ARAGÓN, Á., *et al.*, "Strength and workability of masonry mortars manufactured with ladle furnace slag", *Resources, Conservation and Recycling*, v. 53, n. 11, pp. 645–651, 2009. doi: http://dx.doi.org/10.1016/j.resconrec.2009.04.015.

[8] SIDERIS, K.K.*,* TASSOS, C.*,* CHATZOPOULOS, A., *et al.*, "Mechanical characteristics and durability of self compacting concretes produced with ladle furnace slag", *Construction & Building Materials*, v. 170, pp. 660–667, 2018. doi: http://dx.doi.org/10.1016/j.conbuildmat.2018.03.091.

[9] ZHAO, J.*,* LIU, Q.*,* FANG, K., "Optimization of f-MgO/f-CaO phase in ladle furnace slag by air rapidly cooling", *Materials Letters*, v. 280, pp. 1–4, 2020. doi: http://dx.doi.org/10.1016/j.matlet.2020.128528.

[10] CHOI, S.*,* KIM, J., "Hydration reactivity of calcium-aluminate-based ladle furnace slag powder according to various cooling conditions", *Cement and Concrete Composites*, v. 114, pp. 1–10, 2020. doi: http://dx.doi.org/10.1016/j.cemconcomp.2020.103734.

[11] FANG, K.*,* WANG, D.*,* ZHAO, J., *et al.*, "Utilization of ladle furnace slag as cement partial replacement: Influences on the hy-dration and hardening properties of cement", *Construction & Building Materials*, v. 299, pp. 124265, 2021. doi: http://dx.doi.org/10.1016/j.conbuildmat.2021.124265.

[12] SERJUN, V.Z.*,* MLADENOVIČ, A.*,* MIRTIČ, B., *et al.*, "Recycling of ladle slag in cement composites: Environmental impacts", *Waste Management (New York, N.Y.)*, v. 43, pp. 376–385, 2015. doi: http://dx.doi.org/10.1016/j.wasman.2015.05.006. PubMed PMID: 26008145.

[13] XU, B.*,* YI, Y., "Use of ladle furnace slag containing heavy metals as a binding material in civil engi-neering", *The Science of the Total Environment*, v. 705, pp. 1–9, 2020. doi: http://dx.doi.org/10.1016/j.scitotenv.2019.135854.

[14] LU, T.*,* CHEN, Y.*,* WANG, H., *et al.*, "The influencing factors for volume stability of ladle slag", *Processes (Basel, Switzerland)*, v. 10, n. 1, pp. 92, 2022. doi: http://dx.doi.org/10.3390/pr10010092.

[15] LI, L.*,* LING, T.C.*,* PAN, S.Y., "Environmental benefit assessment of steel slag utilization and carbonation: a systematic review", *The Science of the Total Environment*, v. 806, n. 1, pp. 150280, 2022. doi: http://dx.doi.org/10.1016/j.scitotenv.2021.150280. PubMed PMID: 34560457.

[16] JIN, F., "Sustainable utilization of slags", In: Tsang, D. C., Wang, L. (eds.), *Low Carbon Stabilization and Solidification of Hazardous Wastes*, Amsterdam, Elsevier, pp. 321–341, 2022. doi: http://dx.doi.org/10.1016/B978-0-12-824004-5.00016-5.

[17] FANG, K.*,* ZHAO, J.*,* WANG, D., *et al.*, "Use of ladle furnace slag as supplementary cementitious material before and after modification by rapid air cooling: a comparative study of influence on the properties of blended cement paste", *Construction & Building Materials*, v. 314, pp. 125434, 2022. doi: http://dx.doi.org/10.1016/j.conbuildmat.2021.125434.

[18] ASSOCIAÇÃO BRASILEIRA DE NORMAS TÉCNICAS, *NBR 16605 – Cimento Portland e outros materiais em pó – Determinação da massa específica*, Rio de Janeiro, ABNT, 2017.

[19] ASSOCIAÇÃO BRASILEIRA DE NORMAS TÉCNICAS, *NBR 16606, Cimento Portland – Determinação da pasta de consistência normal*, Rio de Janeiro, ABNT, 2017.

[20] HERRERO, T.*,* VEGAS, I.J.*,* SANTAMARÍA, A., *et al.*, "Effect of high-alumina ladle furnace slag as cement substitution in masonry mortars", *Construction & Building Materials*, v. 123, pp. 404–413, 2016. doi: http://dx.doi.org/10.1016/j.conbuildmat.2016.07.014.

[21] ASSOCIAÇÃO BRASILEIRA DE NORMAS TÉCNICAS, *NBR 13279, Argamassa para assentamento e revestimento de paredes e tetos – Determinação da resistência à tração na flexão e à compressão*, Rio de Janeiro, ABNT, 2005.

[22] ASSOCIAÇÃO BRASILEIRA DE NORMAS TÉCNICAS, *NBR 16697, Cimento Portland – Requisitos,* Rio de Janeiro, ABNT, 2018.

[23] YI, H., XU, G., CHENG, H., *et al.*, "An overview of utilization of steel slag", *Procedia Environmental Sciences*, v. 16, pp. 791–801, 2012. doi: http://dx.doi.org/10.1016/j.proenv.2012.10.108.

[24] SETIÉN, J., HERNÁNDEZ, D., GONZÁLEZ, J.J., "Characterization of ladle furnace basic slag for use as a construction material", *Construction & Building Materials*, v. 23, n. 5, pp. 1788–1794, 2009. doi: http://dx.doi.org/10.1016/j.conbuildmat.2008.10.003.

[25] YILDIRIM, I.Z., PREZZI, M., "Experimental evaluation of EAF ladle steel slag as a geo-fill material: mineralogical, physical e mechanical properties", *Construction & Building Materials*, v. 154, pp. 23–33, 2017. doi: http://dx.doi.org/10.1016/j.conbuildmat.2017.07.149.

[26] HENRÍQUEZ, P.A., APONTE, D., IBÁÑEZ-INSA, J., *et al.*, "Ladle furnace slag as a partial replacement of Portland cement", *Construction & Building Materials*, v. 289, pp. 1–18, 2021.

[27] HAMMAT, S., MENADI, B., KENAI, S., *et al.*, "Properties of self-compacting mortar containing slag with different finenesses", *Civil Engineering Journal*, v. 7, n. 5, pp. 840–856, 2021. doi: http://dx.doi.org/10.28991/cej-2021-03091694.

[28] NAJM, O., EL-HASSAN, H., EL-DIEB, A., "Ladle slag characteristics and use in mortar and concrete: a comprehensive review", *Journal of Cleaner Production*, v. 288, pp. 1–22, 2021. doi: http://dx.doi.org/10.1016/j.jclepro.2020.125584.

[29] FALESCHINI, F., ALEJANDRO FERNÁNDEZ-RUÍZ, M., ZANINI, M.A., *et al.*, "High performance concrete with electric arc furnace slag as aggregate: mechanical and durability properties", *Construction & Building Materials*, v. 101, pp. 113–121, 2015. doi: http://dx.doi.org/10.1016/j.conbuildmat.2015.10.022.

[30] PELLEGRINO, C., CAVAGNIS, P., FALESCHINI, F., *et al.*, "Properties of concretes with black/oxidizing electric arc furnace slag aggregate", *Cement and Concrete Composites*, v. 37, n. 1, pp. 232–240, 2013. doi: http://dx.doi.org/10.1016/j.cemconcomp.2012.09.001.

[31] VILAPLANA, A.S.D.G., FERREIRA, V.J., LÓPEZ-SABIRÓN, A.M., *et al.*, "Utilization of Ladle Furnace slag from a steelwork for laboratory scale production of Portland cement", *Construction & Building Materials*, v. 94, pp. 837–843, 2015. doi: http://dx.doi.org/10.1016/j.conbuildmat.2015.07.075.

[32] LEMOS, B.R.S., "*Oxidação de sulfetos promovida por materiais carbonáceos ativados*", M.Sc. Thesis, Universidade Federal de Minas Gerais, Belo Horizonte, Minas Gerais, 2010.

[33] BRAVO, L.F.R., SILVA, E.R. "*Influência do tempo e da temperatura na oxidação dos aços SAE 1020 E SAE 304*", M.Sc. Thesis, Universidade de Rio Verde, Rio Verde, Goiás, 2017.

[34] MARINHO, A.L., MOL SANTOS, C.M., CARVALHO, J.M.F.D., *et al.*, "Ladle furnace slag as binder for cement-based composites", *Journal of Materials in Civil Engineering*, v. 29, pp. 1–12, 2017.

[35] SHI, C., HU, S., "Cementitious properties of ladle slag fines under autoclave curing conditions", *Cement and Concrete Research*, v. 33, n. 11, pp. 1851–1856, 2003. doi: http://dx.doi.org/10.1016/S0008-8846(03)00211-4.

[36] FRÍAS ROJAS, M., SÁNCHEZ DE ROJAS, M.I., "Chemical assessment of the electric arc furnace slag as construction material: expansive compounds", *Cement and Concrete Research*, v. 34, n. 10, pp. 1881–1888, 2004. doi: http://dx.doi.org/10.1016/j.cemconres.2004.01.029.

[37] YILDIRIM, I.Z., PREZZI, M., "Chemical, mineralogical, and morphological properties of steel slag", *Advances in Civil Engineering*, v. 2011, pp. 1–13, 2011. doi: http://dx.doi.org/10.1155/2011/463638.

[38] ADESANYA, E., OHENOJA, K., KINNUNEN, P., *et al.*, "Properties and durability of alkali-activated ladle slag", *Materials and Structures*, v. 50, n. 6, pp. 1–10, 2017. doi: http://dx.doi.org/10.1617/s11527-017-1125-4.

[39] XU, Q., HU, J., RUIZ, J.M., *et al.*, "Isothermal calorimetry tests and modeling of cement hydration parameters.", *Thermochimica Acta*, v. 499, n. 1–2, pp. 91–99, 2010. doi: http://dx.doi.org/10.1016/j.tca.2009.11.007.

[40] LINDEROTH, O., WADSÖ, L., JANSEN, D., "Long-term cement hydration studies with isothermal calorimetry", *Cement and Concrete Research*, v. 141, pp. 106344, 2021. doi: http://dx.doi.org/10.1016/j.cemconres.2020.106344.

[41] SANTAMARIA, A., ORTEGA-LOPEZ, V., SKAF, M., *et al.*, "Ladle furnace slag as cement replacement in mortar mixes", In: *Proceedings of the Fifth International Conference on Sustainable Construction Materials and Technologies*, Kingston University, London, UK, 14–17 July 2019. doi: http://dx.doi.org/10.18552/2019/IDSCMT5048.

[42] PARRON-RUBIO, M.E.*,* PEREZ-GARCIA, F.*,* GONZALEZ-HERRERA, A., *et al.*, "Slag substitution as a cementing material in concrete: mechanical, physical and environmental properties.", *Materials (Basel)*, v. 12, n. 18, pp. 12, 2019. doi: http://dx.doi.org/10.3390/ma12182845. PubMed PMID: 31487805.

[43] HOPPE FILHO, J., GOBBI, A., PEREIRA, E., *et al.,* "Pozzolanic activity of mineral additions to portland cement (Part I): pozzolanic activity index with lime (PAI), X-ray diffraction (XRD), thermogravimetry (TG/DTG) and modified Chapelle.", *Revista Materia*, v. 22, n. 3, pp. 1–18, 2017.

[44] ALARCON-RUIZ, L.*,* PLATRET, G.*,* MASSIEU, E., *et al.*, "The use of thermal analysis in assessing the effect of temperature on a cement paste.", *Cement and Concrete Research*, v. 35, n. 3, pp. 609–613, 2005. doi: http://dx.doi.org/10.1016/j.cemconres.2004.06.015.

[45] BETIOLI, A. M., "*Influência dos polímeros MHEC e EVA na hidratação e comportamento reológico de pastas de cimento portland*", D.Sc. Thesis, Universidade Federal de Santa Catarina, Florianópolis, Santa Catarina, 2007.

[46] FERREIRA, E. G. A., "*Avaliação da alteração nas propriedades da pasta de cimento em ambiente de repositório*", M.Sc. Thesis, Universidade de São Paulo, São Paulo, São Paulo, 2013.

[47] GALVÃO, S. P., "*Estudo microestrutural de pastas de cimento modificadas por emulsões de base acrílica e acrílica estirenada*", D.Sc. Thesis, Universidade Federal de Pernambuco, Recife, Pernambuco, 2010.

[48] PIZZOL, V. D., "*Carbonatação acelerada nova tecnologia de cura para fibrocimento sem amianto*", M.Sc. Thesis, Universidade Federal de Lavras, Lavras, Minas Gerais, 2013.

[49] VELASCO, R.V.*,* FILHO, R.D.T.*,* CORDEIRO, G.C., *et al.*, "Estudo da Influência da pressão de cura na hidratação de pastas de cimentação por meio de termogravimetria.", *Rio Oil & Gas Expo and Conference*, v. 10, pp. 1–8, 2010.

[50] GUMIERI, A. G., "*Estudo da viabilidade técnica da utilização de escórias de aciaria do processo LD como adição em cimentos*", D.Sc. Thesis, Universidade Federal do Rio Grande do Sul, Porto Alegre, Rio Grande do Sul, 2002.

[51] ROMANO, R.C.O.*,* FUJII, A.L.*,* SOUZA, R.B., et al., "Acompanhamento da hidratação de cimento Portland simples com resíduo de bauxita.", *Cerâmica*, v. 62, n. 363, pp. 215–223, 2016. doi: http://dx.doi.org/10.1590/0366-69132016623632039.